ResearchGate

See discussions, stats, and author profiles for this publication at: https://www.researchgate.net/publication/27265996

Electrochemical Fabrication of Highly Ordered Semiconductor and Metallic Nanowire Arrays

ARTICLE *in* CHEMISTRY OF MATERIALS · AUGUST 2001

Impact Factor: 8.35 · DOI: 10.1021/cm0007297 · Source: OAI

CITATIONS
116

READS
69

7 AUTHORS, INCLUDING:

Bw Zhang
Hunan University
249 PUBLICATIONS **9,497** CITATIONS
SEE PROFILE

Ming Jie Zheng
University of Wisconsin–Madison
42 PUBLICATIONS **667** CITATIONS
SEE PROFILE

Lixia Zhao
Chinese Academy of Sciences
61 PUBLICATIONS **1,326** CITATIONS
SEE PROFILE

Available from: Lixia Zhao
Retrieved on: 01 February 2016

Electrochemical Fabrication of Highly Ordered Semiconductor and Metallic Nanowire Arrays

X. Y. Zhang,* L. D. Zhang, W. Chen, G. W. Meng, M. J. Zheng, and L. X. Zhao

Institute of Solid State Physics, Chinese Academy of Sciences, Hefei 230031 People's Republic of China

F. Phillipp

Max-Planck-Institut für Metallforschung, Heisenbergstrasse 1,D-70569, Stuttgart, Germany

Received September 11, 2000. Revised Manuscript Received May 22, 2001

In this article, we report the fabrication of highly ordered TiO_2 nanowire arrays by anodic oxidative hydrolysis of $TiCl_3$ within a hexagonal close-packed nanochannel alumina (NCA). The single-crystalline anatase TiO_2 nanowires with diameters about 15 nm and lengths about 6 μm are obtained after annealing at 500 °C. Finally, the fabrication and characterization of highly ordered Au and Ni nanowire arrays with selectable diameters are also reported.

Introduction

In recent years, there has been increasing interest in the fabrication of one-dimensional nanostructures because of their potential utilization in electronic, magnetic, optical, and micromechanical devices. The ability to precisely prepare such structures on a large scale is an important goal of materials science. One strategy is to use porous nanochannel alumina (NCA) template to fabricate such structures.[1−4] An important advantage of the template method is that the nanowires prepared in this way can be diameter-controllable and well-defined. TiO_2 is one of the most important semiconductor materials, widely used as a catalyst support,[5] a photocatalyst,[6] in solar cells,[7] and in sensors.[8,9] Meanwhile, metallic nanowires are of great interest from a fundamental point of view as well as for future applications. Highly ordered metallic nanowire arrays are particularly important for obtaining scaled-up functional devices for use as microelectrodes, probes, and data storage devices.[1,10−12]

TiO_2 nanowire arrays have been synthesized using a sol−gel template method.[13] However, the sol−gel method has some disadvantages in preparing such structures; for example, the organic precursors are often hydrolyzed fast and easy to form unstable gel.[14] Electrochemical synthesis is cheap and fast in comparison with the sol−gel method. Nanoporous polycrystalline anatase TiO_2 film has been electrodeposited by a two-step replication process from anodic porous alumina.[15] Here, we report the fabrication of the single-crystalline anatase TiO_2 nanowire arrays by anodic oxidative hydrolysis of $TiCl_3$. The fabrication of Au and Ni nanowire arrays is also reported.

Experimental Section

NCA templates were prepared by means of anodization.[16,17] Briefly, high-purity (99.999%) aluminum foils were used as the starting material. Prior to anodizing, the aluminum was annealed at 500 °C in order to obtain homogeneous conditions for pore growth over large areas. Subsequently, the foils were electropolished in a 1:9 by volume mixture of $HClO_4$ and C_2H_5-OH. Anodization was carried out under a constant cell voltage in an oxalic acid solution. After the anodization, the remaining aluminum was removed in a saturated $HgCl_2$ solution. Then, the pore bottoms were opened and widened by chemical etching in aqueous phosphoric acid. To fabricate the nanowire arrays, a thin layer of Au about 100 nm was deposited as an electrode on one side of the anodic porous alumina template using a vacuum evaporation apparatus.

TiO_2 nanowires were prepared by anodic oxidative hydrolysis of acidic aqueous $TiCl_3$ solutions using the potentiostatic method with a three-electrode arrangement with a saturated calomel reference electrode (SCE) and a Pt counter electrode. Preparation of TiO_2 nanowires was performed from a 0.25 M $TiCl_3$ solution at 25 °C under an Ar atmosphere, pH 2.5. The anode potential was kept at 0.1 V vs SCE. Then, the sample was annealed at 500 °C in order to obtain anatase TiO_2 nanowires. Au nanowires were electrodeposited from the following solution: 12 g/L $HAuCl_4$, 160 g/L Na_2SO_3, 5 g/L

* Corresponding author. E-mail: zxyxlh@mail.hf.ah.cn.

(1) Martin, C. R. *Science* **1994**, *266*, 1961.
(2) Parthasarathy, R. V.; Phani, K. L. N.; Martin, C. R. *Adv. Mater.* **1995**, *7*, 896.
(3) Martin, C. R. *Chem. Mater.* **1996**, *8*, 1739.
(4) Martin, C. R. *Chem. Mater.* **1997**, *9*, 2544.
(5) Matsuda, S. *Appl. Catal.* **1983**, *8*, 149.
(6) Dagan, G.; Tomkiewics, M. *J. Phys. Chem.* **1993**, *97*, 12651.
(7) Bach, U.; Lupo, D.; Comte, P.; Moser, J. E.; Weissortel, F.; Salbeck, J.; Spreitzer, H.; Grätzel, M. *Nature* **1998**, *395*, 583.
(8) Azad, A. M.; Younkman, L. B.; Akbar, S. A. *J. Am. Ceram. Soc.* **1994**, *77*, 481.
(9) Yeh, Y. C.; Tseng, T. T.; Chang, D. A. *J. Am. Ceram. Soc.* **1990**, *73*, 1992.
(10) Whitney, T. M.; Jiang, J. S.; Searson, P. C.; Chien, C. L. *Science* **1993**, *261*, 1316.
(11) Huber, C. A.; Huber, T. E.; Sadoqi, M.; Lubin, J. A.; Manalis, S.; Prater, C. B. *Science* **1994**, *263*, 800.
(12) Uosaki, K.; Okazaki, K.; Kita, H.; Takahashi, H. *Anal. Chem.* **1990**, *62*, 652.
(13) Lakshmi, B. B.; Patrissi, C. J.; Martin, C. R. *Chem. Mater.* **1997**, *9*, 2544.
(14) Mackenzie, J. D. *J. Non-Cryst. Solids* **1982**, *41*, 1.
(15) Hoyer, P.; Masuda, H. *J. Mater. Sci. Lett.* **1996**, *15*, 1228.
(16) Masuda, H.; Fukuda, K. *Science* **1995**, *268*, 1466.
(17) Masuda, H.; Staoh, M. *Jpn. J. Appl. Phys., Part 2* **1996**, *35*, L126.

10.1021/cm0007297 CCC: $20.00 © 2001 American Chemical Society
Published on Web 07/25/2001

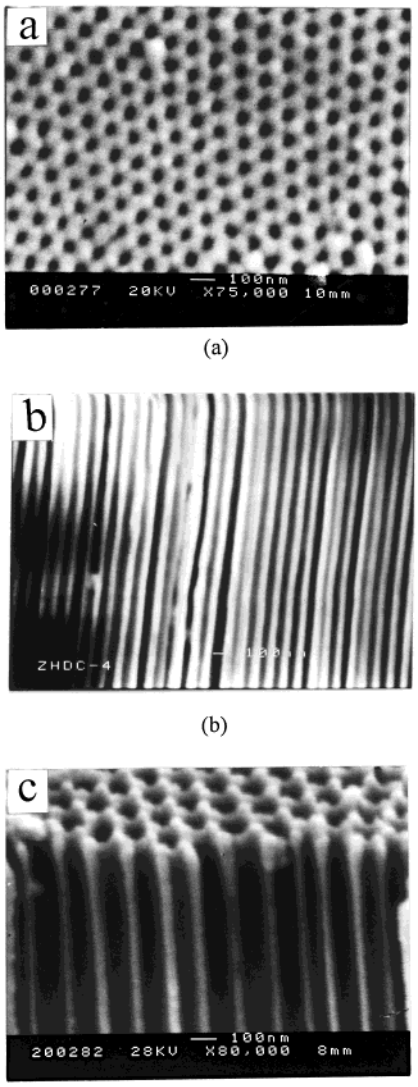

Figure 1. Nanochannel alumina templates: SEM images of porous alumina which was anodized in a 0.3 M oxalic acid at 12 °C at 40 V: (a) view of the surface; (b) cross-sectional view. (c) Oblique cross-sectional view of porous alumina which was anodized in a 0.25 M oxalic acid at 3 °C at 70 V.

EDTA, 30 g/L K_2HPO_4, 0.5 g/L $CoSO_4$; pH 9.0. The cathode current density was kept at 0.5 mA/cm^2, and the temperature of the bath was kept at 45 °C. Ni nanowires were electrodeposited from the following solution: 200 g/L $NiCl_2 \cdot 6H_2O$, 120 g/L $NiSO_4 \cdot 7H_2O$, 50 g/L H_3BO_3; pH 4.2. The cathode current density was kept at 4 mA/cm^2, and the temperature of the bath was maintained at 25 °C.

The structure and morphology of the nanowire arrays were investigated using a scanning electron microscope (SEM, JEOL JSM-6300), a transmission electron microscope (TEM, JEM-200CX), a high-resolution transmission electron microscope (HRTEM, JEOL-2010), and a laser Raman scattering spectrometer (Spex 1403) with a 514.5 nm incident wavelength and a 200 mW output power.

Results and Discussion

NCA Templates. Hexagonal close-packed arrays of porous alumina with selectable diameters ranging from approximately 35 to 100 nm can be formed in oxalic acid solutions by varying anodizing conditions and the time of pore widening treatment. Figure 1 shows the SEM images of hexagonal close-packed arrays of porous alumina. Figure 1a,b shows SEM images of porous alumina which was anodized in a 0.3 M oxalic acid at 12 °C at 40 V. The cross sections of the parallel cylindrical pores can be clearly seen, and the channel diameter and interpore distance are 45 and 105 nm, respectively. Figure 1c shows an oblique cross-sectional view of porous alumina which was anodized in a 0.25 M oxalic acid at 3 °C at 70 V. The channel diameter and the interpore distance are approximately 95 and 135 nm, respectively.

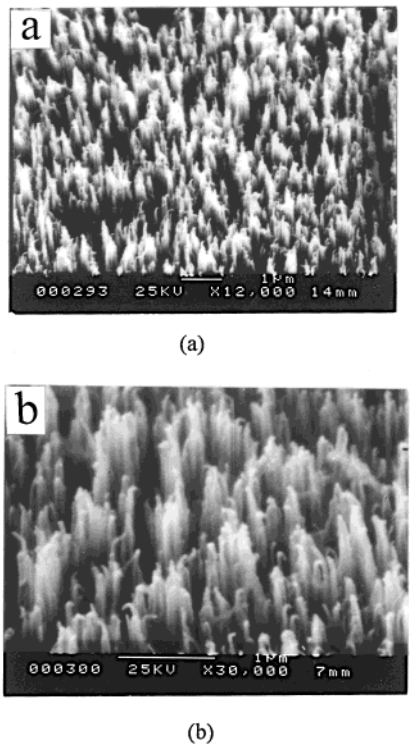

Figure 2. SEM images of the ordered TiO_2 nanowire array: (a) low-magnification image; (b) high-magnification image.

TiO_2 Nanowires. Figure 2 shows the SEM images of the TiO_2 nanowire arrays prepared in the NCA template with diameters of 45 nm, which resulted from etching away the alumina using a mixture of 6 wt % phosphoric acid and 1.8 wt % chromic acid followed by cleaning in an ultrasonic bath. It can be seen that TiO_2 nanowires are of an equal height and have a highly ordered tip array. Most of the nanowire tips are crooked, which should be caused by the etching process. Figure 3a shows the TEM image of a TiO_2 nanowire bundle after partly dissolving away the alumina. The TiO_2 nanowires are straight; the diameters and lengths are about 15 nm and 6 μm, respectively. It is interesting that the diameter of TiO_2 nanowires is much smaller than the pore diameter of alumina template. Figure 3b shows a TEM image of a TiO_2 nanowire located at the center of cylindrical alumina pore. Figure 3c shows the TEM image of a single TiO_2 nanowire after completely dissolving away the alumina. The selected-area electron diffraction (SAED) pattern of the TiO_2 nanowire (Figure 3c, inset) could be indexed as single-crystal anatase TiO_2[110]. The single-crystal structure was further confirmed by high-resolution electron microscopy (HRTEM) images. Figure 3d shows the HRTEM image of a TiO_2 nanowire with ca. 15 nm diameter. This image shows the single-crystal structure of the nanowire and

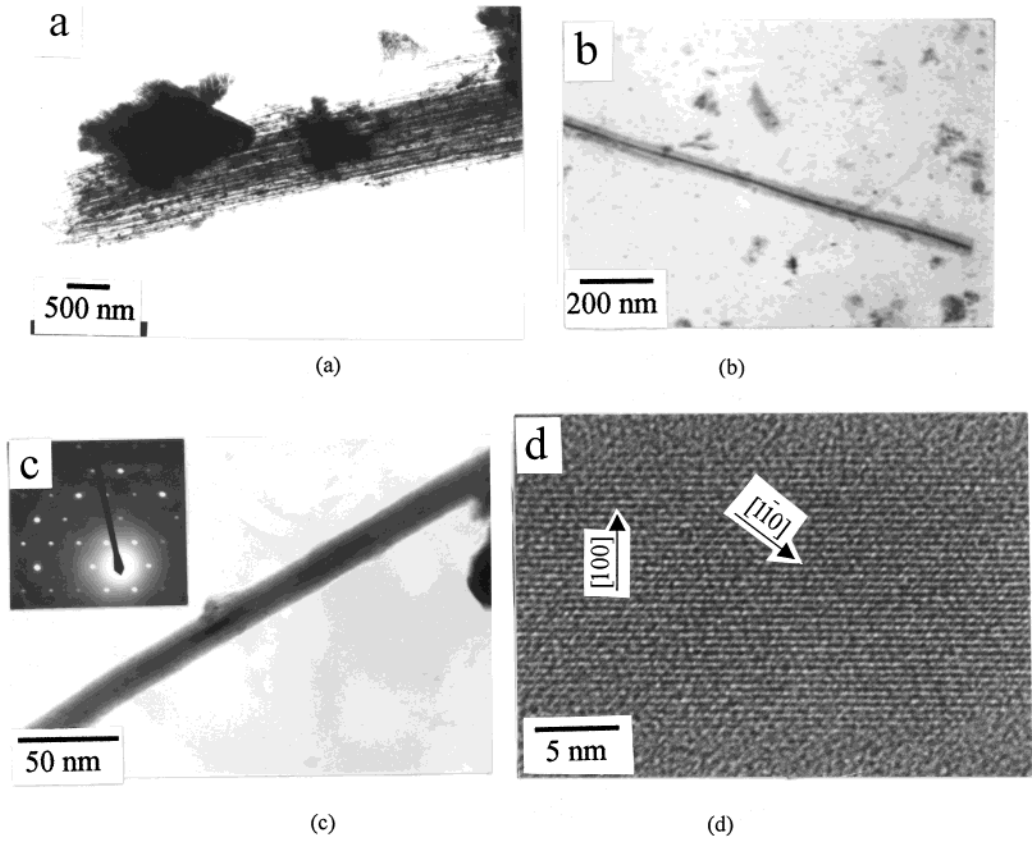

Figure 3. TEM images of the TiO_2 nanowires: (a) TEM image of a TiO_2 nanowire bundle; (b) TEM image of a TiO_2 nanowire located at the center of the cylindrical alumina pore; (c) TEM image of one of the TiO_2 nanowires (the inset shows the SAED pattern of the nanowire); (d) HRTEM image of a single-crystalline TiO_2 nanowire.

the (100) and (1$\bar{1}$0) lattice fringes with interplane spacings of around 0.38 and 0.27 nm, respectively. The (100) lattice plane is the typically observed plane for rodlike anatase nanoparticles.[18] It can be concluded that the nanowires are highly axial oriented.

In the case of nanophase TiO_2, Raman spectroscopy has been employed successfully to elucidate the issues related to phases, phase transformations, and grain boundary structure.[19,20] Figure 4 shows the Raman scattering spectra of TiO_2 nanowire arrays measured at room temperature. The broad bands of the as-deposited nanowire arrays are located around 158, 410, and 626 cm^{-1}, revealing the amorphous character of the sample.[21] After heating at 500 °C,the bands are located at 148, 399, 516, and 640 cm^{-1}, corresponding to the typical Raman peaks of anatase TiO_2.[22] The prominent, intense low-frequency mode at 148 cm^{-1} corresponds to one of the E_g modes, which has been assigned to the O−Ti−O bending vibration.

Preparation of TiO_2 (anatase) films by anodic oxidative hydrolysis of $TiCl_3$ has been reported by Kavan et al. The mechanism of the process was also postulated:[23,24] in the process of anodic oxidative hydrolysis of $TiCl_3$, the rate of anodic Ti^{3+}(aq) oxidation is controlled,

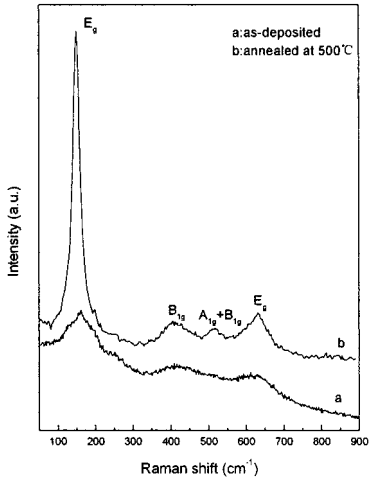

Figure 4. Raman scattering spectra of the TiO_2 nanowire arrays.

analogous to the chemical oxidation with O_2, by a rapid hydrolytic preequilibrium, followed by the oxidation of thus formed $TiOH^{2+}$ monohydroxy intermediate to Ti(IV) oxo species. This consists probably of partly dehydrated (cross-linked) polymeric titanium(IV) hydroxide, containing both terminal and bridged OH groups. This material is converted finally into TiO_2 by annealing. At this stage, the situation is quite different by the presence of the NCA template. An explanation of the

(18) Burnside, S. D.; Shklover, V.; Barbé, C.; Comte, P.; Arendse, F.; Brooks, K.; Grätzel, M. *Chem. Mater.* **1998**, *10*, 2419.
(19) Melendres, C. A.; Narayanasamy, A.; Maroni, V. A.; Siegel, R. W. *J. Mater. Res.* **1989**, *4*, 1246.
(20) Paker, J. C.; Siegel, R. W. *J. Mater. Res.* **1990**, *5*, 1246.
(21) Hsu, L. S.; Rujkorakarn, R.; Sites, J. R.; She, C. Y. *J. Appl. Phys.* **1986**, *59*, 3475.
(22) Ohsaka, T.; Izumi, F.; Fujiki, Y. *J. Raman Spectrosc.* **1978**, *7*, 221.
(23) Kavan, L.; Stoto, T.; Grätzel, M.; Fitzmzurice, D.; Shklover, V. *J. Phys. Chem.* **1993**, *97*, 9493.
(24) Kavan, L.; O'Regan, B.; Kay, A.; Grätzel, M. *J. Electroanal. Chem.* **1993**, *346*, 291.

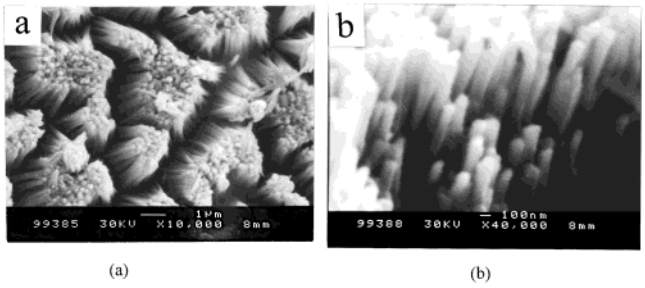

Figure 5. SEM images of the ordered Au nanowire array: (a) low-magnification image; (b) high-magnification image.

nanowire growth mechanism within the NCA template must remain speculative. According to the observations of SEM and TEM, the nanowires nucleate and grow at the center of the alumina pore. As we know, there are many oxygen vacancies on the pore walls, so the pore walls of the alumina template are positively charged.[25] It can be inferred that $TiOH^{2+}$ particles could be repelled by the electric field of the pore walls when they enter the pores. Therefore, we tentatively suggest that the repulsion of the electric field of the pore walls might be responsible for the nucleation of the nanowires at the center of the alumina pores. In an electrochemical cell, anions migrate toward the anode and cations toward the cathode under the action of applied electric field. In the process of anodic oxidative hydrolysis, the transport of $TiOH^{2+}$ acts contrary to the action of the applied electric field. Therefore, the transport of $TiOH^{2+}$ from the bulk electrolyte to the anode/solution interface is only caused by the concentration difference between the bulk electrolyte and the interface. Furthermore, the rate of diffusion of ions in the pores is slower than on the plane surface. Considering the high resistance of the solution in the pores, we used a 0.25 M $TiCl_3$ solution; the concentration is much higher than that for preparing TiO_2 films.[23] According to the observations of Raman spectra, the as-deposited nanowires are amorphous. This amorphous material is converted into anatase TiO_2 and the diameter of the nanowires decreases greatly during the heat treatment.[23] It is well-known that the oriented growth of nanowires within the template can lead to the formation of single-crystal nanowires.[26,27] Single-crystal oriented anatase TiO_2 nanowires within the NCA template have been prepared by a sol−gel method.[13] In our experiments, the observations of HRTEM show that the nanowires are highly axial oriented. Therefore, we suggest that the preferred orientation growth of the TiO_2 nanowires within the channel pores should account for the formation of single-crystalline anatase TiO_2 nanowires.

Au Nanowires. Figure 5 shows the SEM images of highly ordered Au nanowire arrays prepared in the NCA template with 95 nm diameter pores. Clearly, the exposed Au nanowires retain the size and shape of the pore in the template. Figure 6a shows the TEM image of the Au nanowires, which is prepared in the NCA template with 45 nm diameter pores. It can be seen that the Au nanowire appears in black. Figure 6b shows the TEM image of a single Au nanowire; the SAED pattern (Figure 6b, inset) of the nanowire could be indexed for the [110] zone axis of single-crystal Au. The single-crystal structure was further confirmed by HRTEM images of the nanowires. The HRTEM image shown in Figure 6c shows clearly the single-crystal structure of

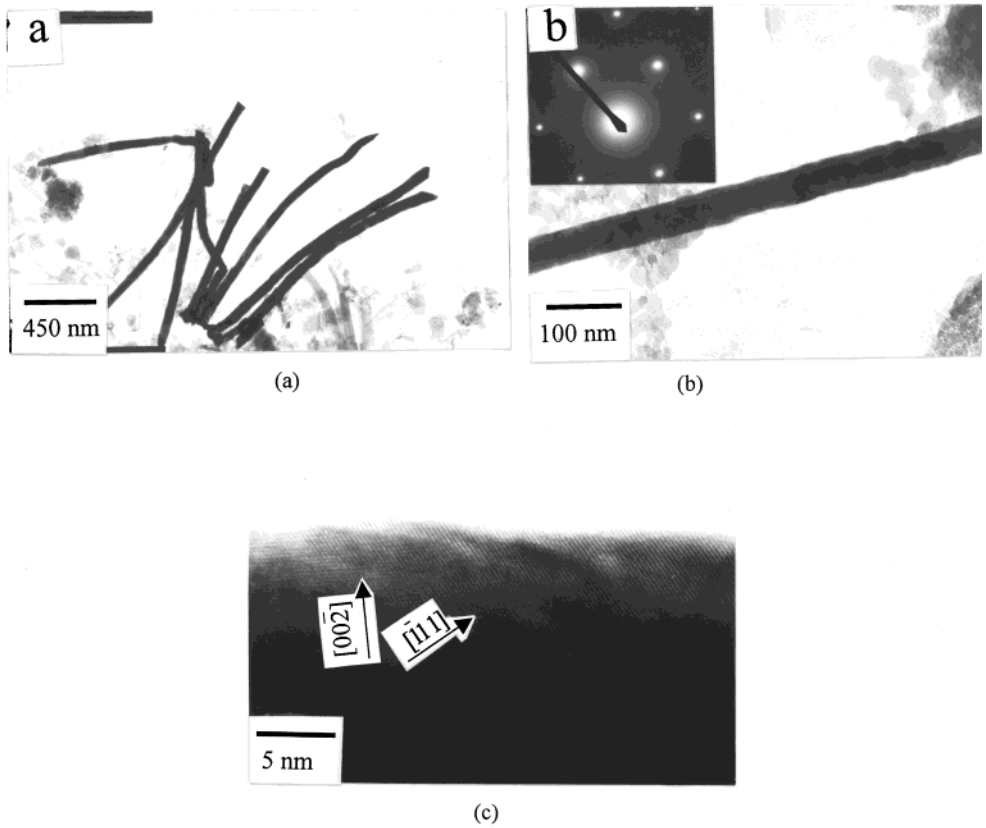

Figure 6. (a) TEM image of an Au nanowire bundle; (b) TEM image of one of the Au nanowires (the inset shows the SAED pattern of the nanowire); (c) HRTEM image of a single-crystalline Au nanowire.

a nanowire and the $(\bar{1}11)$ and $(00\bar{2})$ lattice fringes with interplane spacings of around 0.24 and 0.20 nm, respectively. It can be seen that only the edge of the nanowire is visible because the central part of the nanowire is too thick to be transmitted by the electron beam.

Ni Nanowires. Figure 7a shows the SEM image of well-aligned Ni nanowire arrays prepared in the NCA template with 95 nm diameter pores. It can be clearly seen that Ni nanowires are of an equal height and have a highly ordered tip array. In most cases, the diameter of Ni nanowires appears larger than the diameter of alumina pores because of the aggregation of Ni nanowires. Figure 7b shows the TEM image of a Ni nanowire bundle, which is prepared in the NCA template with 45 nm diameter pores. The Ni nanowires are straight and have uniform diameters about 45 nm. The SAED pattern of one of the nanowires is shown in Figure 7c. It can be concluded from the observation that the nanowires are typical polycrystals.

It is worth noting that the structures differ between the Au nanowires and Ni nanowires. The character of metal and the electrodepostion condition have a great influence on the electrodeposition of metal. In order to deposit single-crystal nanowires, the deposition process is expected to approach an equilibrium process, the distribution of the growth rate of a crystal on the epitaxial interface should be homogeneous, and the formation of new crystal nucleus must be avoided in the electrodeposition process. It can be inferred that a small stable cathode current density is essential to approach an equilibrium state. In our experiment, the current density of deposition of Au is much lower than that of deposition of Ni. Besides, the character of the metal and content of the electrolyte also influence the structure of the nanowires. All of these should be responsible for the structural difference between the Au nanowires and Ni nanowires. Determining the exact nature of the deposition process will require further detailed study.

Conclusions

Highly ordered TiO_2, Au, and Ni nanowire arrays have been electrochemically fabricated within hexagonal close-packed nanochannel alumina (NCA) templates with selectable channel diameters ranging from approximately 35 to 100 nm. The gentle electrochemical fabrication method presented is fast and inexpensive. These highly ordered semiconductor and metallic nanowire arrays would be useful for study of the material properties of nanowires and have potential utilization in the future.

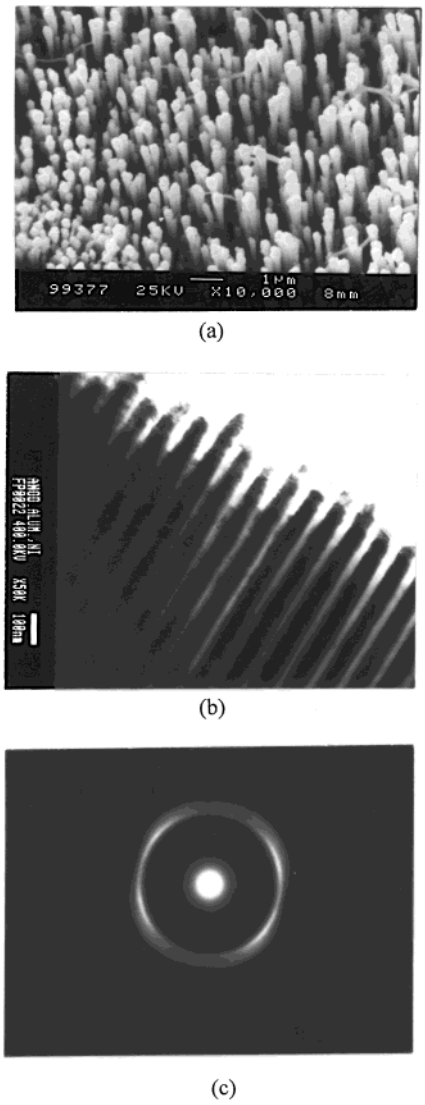

Figure 7. Ni nanowire arrays: (a) SEM image of the ordered Ni nanowire array; (b) TEM image of the ordered Ni nanowire array; (c) SAED pattern of one of the nanowires.

Acknowledgment. The authors thank Professor S. Y. Zhang and Professor G. H. Li for valuable discussions. The financial support of this work by the Key Project of National Fundamental Research of China and the Natural Science Foundation of China (Grant No. 19974055) is acknowledged.

CM0007297

(25) Diggle, J. W.; Downie, T. C.; Goulding, C. W. *Chem. Rev.* **1969**, *69*, 365.
(26) Dubois, S.; Michel, A.; Eymery, J. P.; Duvail, J. L.; Piraux, L. *J. Mater. Res.* **1999**, *14*, 665.
(27) Xu, D.; Xu, Y.; Chen, D.; Guo, G.; Gui, L.; Tang, Y. *Adv. Mater.* **2000**, *12*, 520.